

PRODUCTION AND CHARACTERIZATION OF PRECIPITATED SILICA FROM PALM OIL MILL FLY ASH USING CO₂ IMPREGNATION AND MECHANICAL FRAGMENTATION

Panca S. Utama¹, Ram Yamsaengsung^{2*} and Chayanoot Sangwichien²

¹ Universitas Riau, Faculty of Engineering, Chemical Engineering Department, Pekanbaru, Indonesia. ORCID: 0000-0002-6829-1321

² Prince of Songkla University, Faculty of Engineering, Chemical Engineering Department, Hatyai, Thailand.
E-mail: ram.y@psu.ac.th, ORCID: 0000-0001-8380-7560

(Submitted: August 26, 2017 ; Revised: December 15, 2017 ; Accepted: January 30, 2018)

Abstract - In this research, sol-gel precipitation using CO₂ impregnation and mechanical fragmentation method was applied to produce precipitated silica from Palm Oil Mill Fly Ash (POMFA). Carbon dioxide (CO₂) was used in order to reduce the cost of the process and to enable sodium hydroxide recovery. The precipitation process was done in a stirred temperature-controlled baffled glass precipitator. The response surface method with the central composite design was applied to optimize the stirring speed and the CO₂ flow rate. The pH and the temperature of the precipitation process were varied for tailoring the specific surface area of the precipitated silica. The mechanical fragmentation and wet crushing process were applied to control the agglomerate particle size of the precipitated silica obtained. The results show that precipitated silica with a specific surface area in the range of 50 – 140 m²/g can be obtained.

Keywords: Carbon dioxide; Mechanical fragmentation; Palm oil mill fly ash; Precipitated silica; Sol-gel precipitation.

INTRODUCTION

The market of synthetic amorphous silica, including silica sol, silica gel, precipitated silica and fume silica, has grown rapidly. In 2015, about 70% of the synthetic amorphous silica demand was for precipitated silica. Precipitated silica is widely used in many industries, with the largest volume being used in rubber and plastic industries as reinforced filler. It is predicted that, in 2018, the valuation of the global precipitated silica market will be \$7 billion USD (Future Market Insights, 2015). To produce high quality amorphous silica, the alkaline extraction method for silica production from silica-containing agricultural waste is generally used. Raw materials such as rice husk ash (Kamath and Proctor, 1998; Kalapathy et al., 2000; Krishnamoorthy et al., 2015), oat husk ash (Zenukhova et al., 2006),

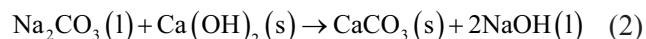
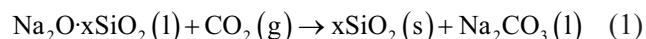
sugar cane bagasse ash (Affandi et al., 2009; Amin et al., 2016) and corn cob ash (Shim et al., 2015) have been used to produce amorphous silica.

Recently, there have been a number of developments of amorphous silica products from biological sources into value-added products. For example, amorphous silica derived from *Panicum milianare* husks ash was modified using a magnesiothermic process to produce uniform mesoporous silicon (Srinivasan et al., 2015). Likewise, surface silica aerogel from fly ash acid sludge was modified using trimethylchlorosilane (TMCS) via solvent exchange and surface modification to obtain a higher specific surface area (SSA) product with lower density and larger pore volume (Cheng et al., 2016). In addition, wet silica aerogel micro-particles obtained from rice husk ash were modified using a sol-gel process in water-in-oil emulsion and dried

* Corresponding author: Ram Yamsaengsung - E-mail: ram.y@psu.ac.th

via supercritical CO₂ to produce products for a drug delivery process (Rajanna et al., 2015).

One of the potential agricultural silica-containing wastes in Southeast Asia is Palm Oil Mill Fly Ash (POMFA). Palm oil production in South East Asia in 2014 was 54,800 million tons (Indexmundi, 2016). The solid waste consists of fiber, shell and empty fruit bunches. Around 85% fiber and 15% shell were used as fuel for boiler with 5 % of the fuel being left unburned and generating ash (Tay and Show, 1995). Thus, it can be estimated that the ash production in 2014 was 3.014 billion tons. In the authors' previous work, alkaline extraction and mechanical fragmentation in sol-gel precipitation using sulfuric acid were applied to produce precipitated silica from POMFA. The extraction kinetics and the effect of the mechanical fragmentation time on the particle size were studied (Utama et al., 2016). However, the use of sulfuric acid in sol-gel precipitation made the process need a large amount of chemicals, which made the process expensive (Rozainee et al., 2008). In this work, carbon dioxide (CO₂) was used to destabilize the silica extract in order to enable sodium hydroxide recovery, which can reduce the amount of chemicals needed for the process. The use of CO₂ in the sol-gel precipitation process produces sodium carbonate in the filtrate of the precipitation process. The sodium carbonate can be converted to sodium hydroxide using calcium hydroxide (Subukhrisna et al. 2007). The reaction of the precipitation process and the sodium hydroxide recovery can be written as follows:



Furthermore, the particle size distribution (PSD) of the precipitated silica agglomerate obtained in the previous work was bimodal. In this work, after the filtration process, the precipitated silica cake was blended with distilled water in a household blender in order to obtain a more uniform particle size and to wash the precipitated silica simultaneously. In summary, the contributions of this work are described as follows:

- The process enables the tailoring of the specific surface area of the precipitated silica.
- The process enables the recovery of the sodium hydroxide used in the extraction process.
- The process can produce a uni-modal precipitated silica particle size distribution.
- The process can produce mesopore precipitated silica which comes in compacted uniform spheres of fairly regular array.

MATERIALS AND METHODS

Materials

The POMFA, having the composition of 30.44% carbon and 39.02% silica from Sawee Industrial Palm Oil Ltd., Chumporn, Thailand, was extracted using 1.4 N sodium hydroxide at the temperature of 105 °C for 60 min. The mass of POMFA to NaOH volume ratio of 0.2341 g/cm³ and the stirring speed of 1065 RPM were used in the extraction process. The silica extract has a silica content of 5.5% (m/v), while the silica to Na₂O mol ratio was 1.1 (Utama et al, 2016). The industrial grade carbon dioxide of 99.5% purity was used as the precipitating agent.

Methods

The precipitation was done in a temperature-controlled baffled glass precipitator (H=D=100 mm) and stirred by a 5 cm four-blade 45 degree pitch turbine type stirrer. The CO₂ was fed into the precipitator by a nozzle. The precipitator was filled with 600 cm³ of the silica extract. The CO₂ flow rate (low =150 cm³/min; high =450 cm³/min) and the stirring speed (low =500 RPM; high = 1000 RPM) were varied. The operating conditions above were chosen because, in that range, visually the CO₂ bubbles were well dispersed in the silica extract. The response surface method (RSM) with central composite design (CCD) was applied to optimize the process. The time required until the gel formed was used to calculate the volume of CO₂ needed for the precipitation process. After the gel formed, the flow of CO₂ was stopped and the stirring speed was increased to 1160 RPM. The methodology and operating conditions used for sol-gel precipitation and the mechanical fragmentation process were adapted from the literature (Cai et al. 2009; Quarch et al., 2010; Utama et al., 2016). At the temperature of 30°C, the pH was varied from 9.5 to 8.0. At the optimum pH, the temperature was varied from 30 to 90°C. At the temperature of 30°C, the pH of 9.5 and the mechanical fragmentation time of 100 min, the particle size distribution (PSD) of the precipitated silica was analysed using the Laser Diffraction Particle Size Analyzer (LPSA), Coulter LS320. The precipitated silica and the liquor were separated using a vacuum filter (EYELA A-3S). The cake was mixed with 1000 cm³ of distilled water and crushed using a 2000 cm³ household blender (AJ BL001). At 5 min interval, 15 cm³ of sample was taken out and the particle size was measured using the LPSA. Next, the precipitated silica was separated from the solution using a vacuum filter before being washed and dried. The specific surface area (SSA) of the precipitated silica were obtained by the Brunauer-Emmett-Teller (BET) method using a surface area analyzer (Quantachrome Nova 2000 e, USA). The physical morphology of the precipitated

silica was determined by a scanning electron microscope (JEOL JSM-5800LV, Japan). The FTIR (Vertex 70, Bruker, USA) was used to identify the chemical bonds in the product. The elemental analysis of the precipitated silica product was conducted by the energy-dispersive X-ray (EDX) method using an SEM EDX (JEOL JSM-5800LV, Japan) and XRF (PW 2400 Philips, Netherland). The X-Ray diffraction (XRD) measurements were carried out with an X-ray Diffractometer (Philips X'Pert MPD, Philips, Netherland) to confirm that the product was in the amorphous form.

Statistical analysis

The RSM-CCD with the full factorial design of 4 cube points, 4 axial points and 5 center points in cube was used to optimize the process. The second order polynomial equation was used to fit the experimental data. The model for the response (η) was:

$$\eta = \beta_0 + \beta_1 x_1 + \beta_2 x_2 + \beta_{11} x_1^2 + \beta_{22} x_2^2 + \beta_{12} x_1 x_2 + \varepsilon \quad (3)$$

where η : CO₂ used (cm³), β_0 (constant term), β_1 and β_2 (linear effects), β_{11} and β_{22} (quadratic effects), β_{12} and β_{13} (interaction effects), x_1 : stirring speed (RPM), x_2 : CO₂ flow rate (cm³/min) and ε : random error. The regression analysis, ANOVA and optimization process were done using Minitab 16.1.1. ANOVA was used to test the compatibility of the model with the experimental data. The Lack of Fit (LoF) test was used to investigate the adequacy of the model (Montgomery, 2001). The optimum condition was verified by conducting experiments at that condition. Responses were monitored and results were compared with model predictions (Ramos-de-la-Pena et al., 2012).

RESULTS AND DISCUSSION

The effect of the CO₂ flow rate and the stirring speed on the volume of CO₂ required for the precipitation process is shown in Table 1. From the results, it can be seen that increasing the CO₂ flow rate and the stirring speed reduces the time required to reach the gel point. It is most likely that the rate-determining step of the CO₂ absorption into the sodium silicate solution in the stirred precipitator is the mass transfer processes from gas to bulk liquid. On the other hand, increasing the stirring speed enhanced the breaking up of the bubbles and makes the size of the bubbles smaller. The smaller bubbles increase the gas-liquid contact area and make the rate of mass transfer increase. This result aligns with the findings of Sardeing et al. (2004), which suggested that the rate of the CO₂ absorption increases with increasing CO₂ flow rate because of larger gas hold up and the gas-liquid contact surface area.

Table 1. Extraction variables and experimental data.

Run No. ^a	Pt Type	Variables		Time Required (min)	Volume of CO ₂ used (cm ³)
		Stirring Speed (RPM) x_1	CO ₂ Flow rate (cm ³ /min) x_2		
1	0	750	300	28.87	8662
2	0	750	300	28.41	8524
3	1	1000	450	14.76	6641
4	0	750	300	28.31	8492
5	1	500	150	65.00	9750
6	-1	396	300	52.97	15892
7	1	500	450	34.99	15746
8	-1	1104	300	22.07	6621
9	0	750	300	28.60	8580
10	0	750	300	28.70	8611
11	1	1000	150	38.80	5820
12	-1	750	512	19.41	9940
13	-1	750	88	60.01	5273

^a Treatments are run in random order.

The regression coefficient and the analysis of variance, which can be used to determine the significance of each regression coefficient and the variables, are shown in Table 2.

It can be seen that all the variables and the regression coefficients gave significant effects on the response variable. The lack of fit test gave a p-value of 0.495 ($p > 0.05$). So there is no evidence that the model proposed does not adequately explain the variation of the response. From the optimization process using the Minitab 16.1.1 software, the optimum condition for destabilizing the silica extract was at a stirring speed of 882 RPM and a CO₂ flow rate of 88 cm³/min. The predictive result of the CO₂ required to reach the gel point (pH 9.5) was 4882 cm³, which fell within the range of the laboratory experimental validation which was 4886±56 cm³.

The application of the mechanical fragmentation process for breaking up the gel and controlling the size of the agglomerate resulted in precipitated silica with

Table 2. Significance of regression coefficients for silica conversion (%) and ANOVA.

Source	Variable constant	Regression Coefficient	p values
Regression			0.000 ^a
Linear			0.000 ^a
	β_0	17587.7	0.000 ^a
x_1	β_1	-35.2627	0.000 ^a
x_2	β_2	49.5651	0.000 ^a
Square			0.000 ^a
x_1^2	β_{11}	0.02169	0.000 ^a
x_2^2	β_{22}	-0.02085	0.000 ^a
Interaction			0.000 ^a
$x_1 x_2$	β_{12}	-0.03450	0.000 ^a
Residual error			
Lack of Fit			0.495

R-Sq = 99.18% R-Sq(pred) = 96.74% R-Sq(adj) = 98.60%.

^a significance at $\alpha = 0.05$.

a mean volume weighed diameter (d_{50}) of $116.25 \pm 4.41 \mu\text{m}$ using a stirring speed of 1160 RPM for 100 min. This result is in accordance with the d_{50} from the previous work, which was $114.7 \mu\text{m}$ at the same stirring speed and time, and the work of Quarch et al. (2010) under a similar condition which was $100 \mu\text{m}$. According to Schlomach and Kind (2004), the destruction of the gel by mechanical force was followed by re-arrangement and compaction of agglomerates, resulting in a final diameter of silica fragments in the range of $30 - 130 \mu\text{m}$. The PSD of the precipitated silica obtained was bimodal. The plot of the d_{50} of the precipitated silica versus time and the comparison of the PSD before and after crushing are depicted in Figures 1 and 2, respectively.

Figure 1 shows the comparison of the PSD of the precipitated silica obtained from mechanical fragmentation and compaction before and after crushing. The crushing process using a household blender for 25 min effectively reduced the agglomerate

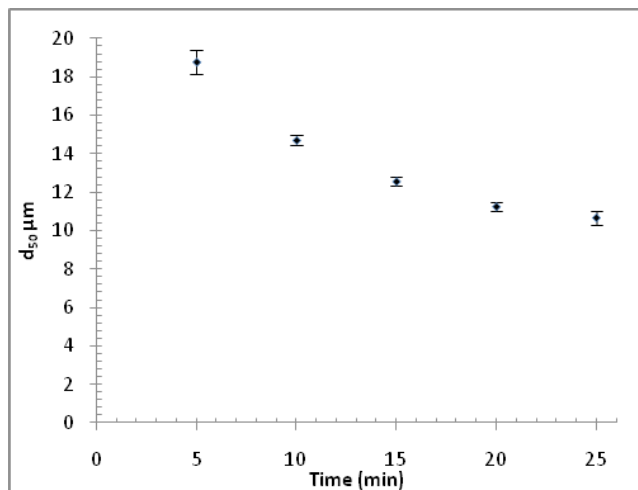


Figure 1. The plot of d_{50} of the precipitated silica versus time.

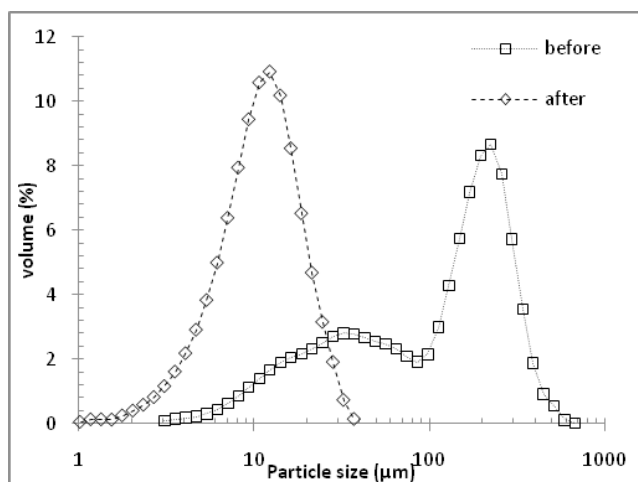


Figure 2. The comparison of the precipitated silica PSD before and after crushing.

of precipitated silica into $10.67 \pm 1.44 \mu\text{m}$ size and made the PSD uni-modal. Figure 2 shows that a crushing time of 5 min can reduce the d_{50} to $18.77 \pm 2.57 \mu\text{m}$, while continued crushing for more than 15 min resulted in less drastic reduction of d_{50} into even smaller sizes.

The effect of the pH and the temperature on the specific surface area (SSA) of the precipitated silica obtained are depicted in Figures 3 and 4, respectively.

From Figure 3, decreasing the pH from 8.75 to 8.30 significantly decreased the SSA of the precipitated silica obtained from $140.75 \text{ m}^2/\text{g}$ to $79.91 \text{ m}^2/\text{g}$. The SSA was closely related to the primary particle size; the smaller the primary particle size, the larger the specific surface area of the precipitated silica obtained. According to Baldyga et al. (2012), the pH of the precipitation process has a significant effect on the aggregation rate. Increasing the pH to a certain range decreases the aggregation rate, so that the resulting particle size becomes smaller.

In Figure 4, increasing the temperature decreases the SSA of the precipitated silica. This result is

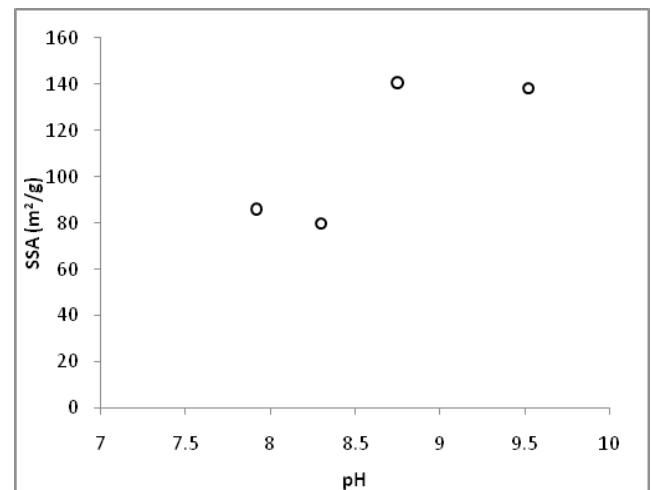


Figure 3. The effect of the pH on the SSA of the precipitated silica at temperature of 30°C .

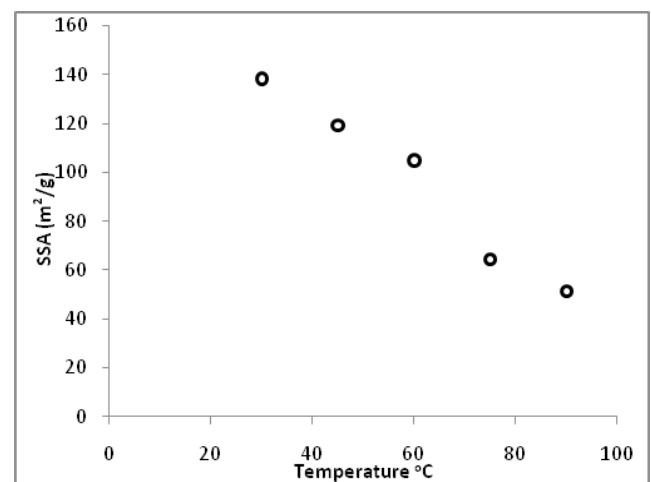


Figure 4. The effect of the temperature on the SSA of the precipitated silica at pH of 9.5.

consistent with Cai et al. (2009) who suggested that higher temperatures increase the nuclei growth with the resulting particle size becoming larger and the SSA of the precipitated silica becoming smaller. The SSA of the precipitated silica obtained was in the range of 50–140 m²/g, which is suitable for reinforcing rubber filler product, such as shoe soles and mechanical rubber goods. Finally, the precipitated silica obtained at the temperature of 30°C and pH of 9.5 was characterized to investigate the physical and the chemical properties.

Figure 5 depicts the micrograph of the precipitated silica using the SEM at magnification of 30,000 times. It is shown that the form of and the size of the primary particle are quite uniform. The primary particle size measured from the SEM image using software ImageJ 1.49v was 58.96±5.40 nm. This result is in accordance with the average primary particle size of the amorphous silica obtained from corn cob ash reported by Shim et al. (2015), which was 60 nm. The SSA of the typical precipitated silica obtained in the conditions mentioned above was 138 m²/g.

Figure 6 illustrates the isotherm of nitrogen adsorption-desorption of the typical precipitated silica obtained. The characteristic of the nitrogen adsorption isotherm and the hysteresis loop is in accordance with a type IV isotherm and the hysteresis loop of type H1 of the IUPAC classification. This can be associated with mesopore materials which are approximately uniform spheres in a fairly regular array (Sing et al., 1985).

The FTIR spectrum of the typical precipitated silica obtained is presented in Figure 7 showing five main IR bands in the spectrum. The 471 cm⁻¹ and the 800 cm⁻¹ IR bands are associated with O-Si-O bending vibrations and the Si-O-Si symmetric stretching vibrations, respectively. The sharp and strong IR band

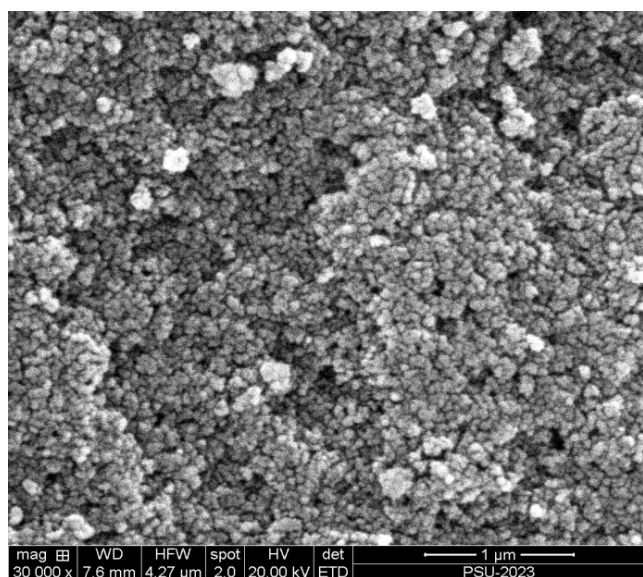


Figure 5. The SEM of the precipitated silica.

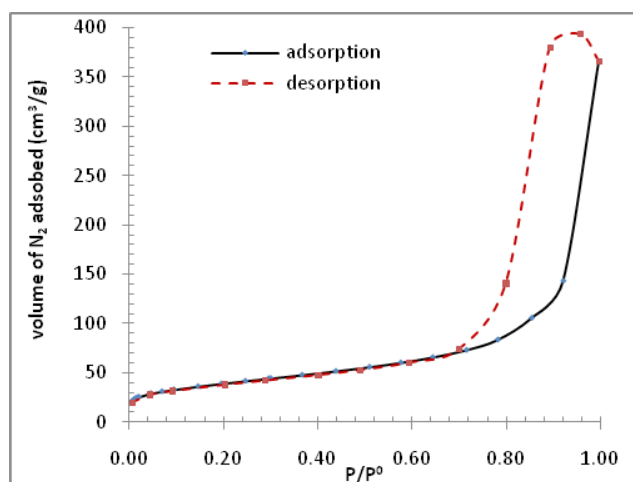


Figure 6. The isotherm of nitrogen adsorption-desorption.

at 1107 cm⁻¹ is due to the Si-O-Si asymmetric stretching vibration. The 1641 cm⁻¹ and the 3452 cm⁻¹ IR bands are due to bending vibrations and stretching vibrations of the water molecule, respectively. The FTIR spectrum of the precipitated silica obtained agrees well with the FTIR spectrum of amorphous silica produced from commercial sodium silicate precipitates using sulfuric acid (Music et al., 2011) and amorphous silica powder obtained by the carbonation method (Cai et al., 2009).

Furthermore, Figure 8 presents the XRD pattern of the precipitated silica obtained. There is no sharp peak, indicating that there is no crystalline material in the precipitated silica. The XRD pattern of the amorphous material has the characteristic of having a broad hump between 15 to 35° of the Bragg angle 2θ (Kamath and Proctor, 1998). The peak of the broad hump recorded in the XRD pattern is the same as the amorphous silica obtained by sol-gel procedure reported by Martinez et al. (2006), which has an amorphous peak at Bragg angle 2θ = 23 degrees.

The SEM-EDS spectrum in Figure 9 shows the impurities of the precipitated silica obtained. There are

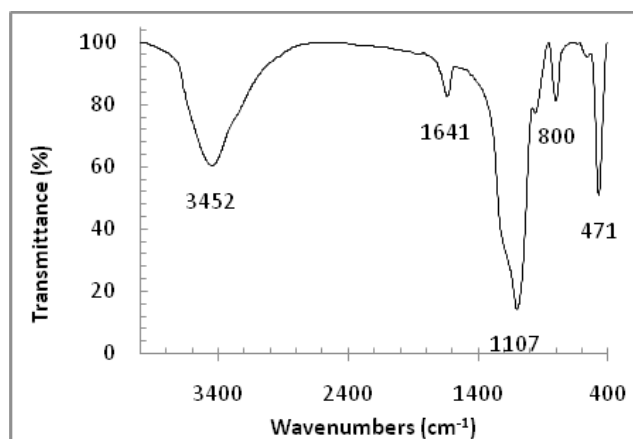


Figure 7. FTIR spectrum of the precipitated silica obtained.

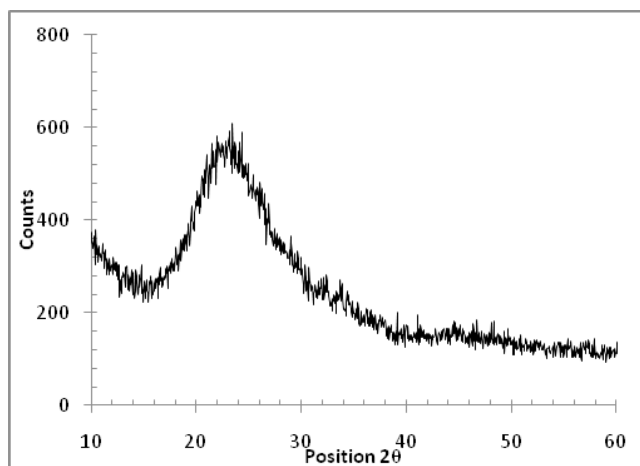


Figure 8. XRD pattern of the precipitated silica.

four elements of impurities found in the precipitated silica: C, K, Al and Na. The elements K and Al were found in the POMFA. The C element was found in the carbonate form in the POMFA and in the precipitation process when CO_2 is dissolved in the silica extract to form the carbonate compound. There was a small amount of these elements carried over into the precipitated silica.

The results of semi-quantitative XRF analysis confirm the elements that were identified in the SEM-EDS spectra. The chemical composition of the precipitated silica analyzed using XRF is shown in Table 3.

It can be seen that the C element was not identified. In XRF analysis, the precipitated silica was heated in a furnace up to 1000 °C before analysis and made the carbonate decompose to carbon dioxide. The purity

Table 3. Chemical composition of the precipitated silica product.

No	Oxide	Weight ^a (%)	Standard (Roemp, 2001)
1	SiO_2	96.90±0.21	≥ 95
2	Na_2O	1.59±0.10	0.2-2.4
4	Al_2O_3	0.46±0.06	-
5	K_2O	1.29±0.14	-
7	LOI	7.12±1.85	2-15

^a mean of triplicate determination

of the precipitated silica obtained of 96.90±0.21% is in the range of standard commercial precipitated silica. The purity of precipitated silica obtained in this process is slightly higher and the impurities are fewer compare to the precipitated silica obtained by sulfuric acid sol-gel precipitation. The purity of precipitated silica obtained by sulfuric acid sol-gel precipitation was 94.92±0.12% and the impurities were: K, Al, Na, Fe and S (Utama et al., 2016). The higher purity and fewer impurities might be because, in this process, the precipitated silica was wet crushed using a blender and the particle size reduced after the sol-gel precipitation process. The wet crush process released the impurities which were trapped in the agglomerate and made the washing process more effective.

Considering the results, the sol-gel precipitation process using CO_2 impregnation and mechanical fragmentation, combined with the alkaline extraction process, shows great promise to be developed to produce precipitated silica from waste of commercial crops, not only POMFA but also sugar cane ash, rice husk ash, corn ash and other siliceous containing ash. This process can be applied to produce precipitated

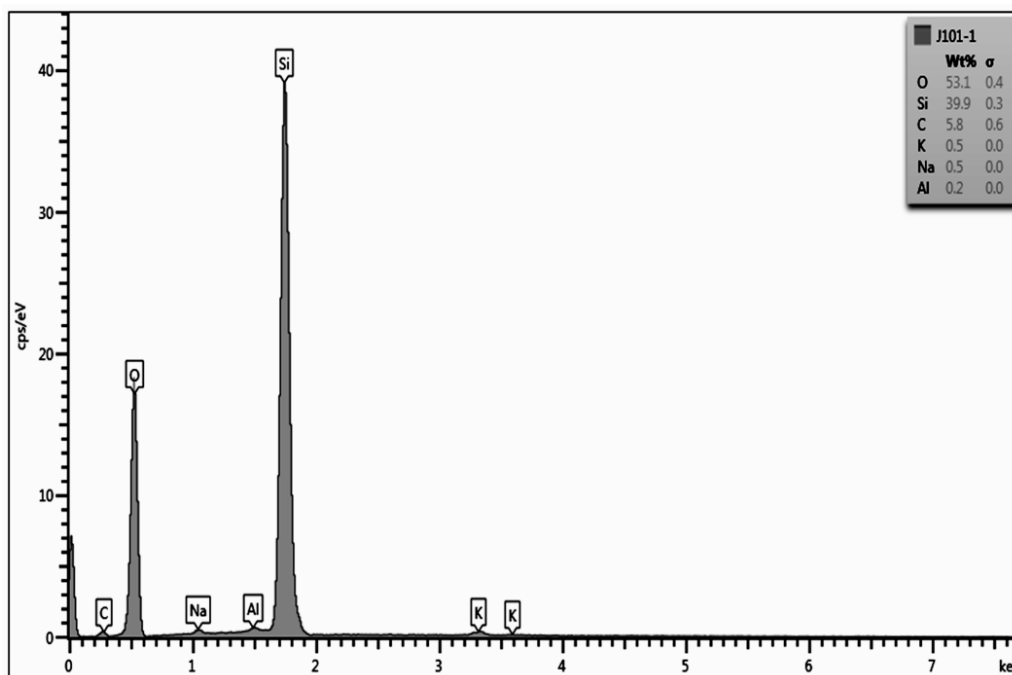


Figure 9. The SEM-EDS spectrum of the precipitated silica.

silica from silica extract with low silica to sodium oxide ratio and the specific surface area of the product can be tailored by varying the pH and temperature of the precipitation process. Moreover, with the sodium hydroxide recovery process, the process might be economically viable. In the alkaline extraction combined with sulfuric acid, sol-gel precipitation need large amounts of sodium hydroxide and sulfuric acid made the process hard to compete with the conventional precipitated silica production from silica sand and soda ash. From the previous work and this work, it can be estimated that, from 1 kg of POMFA, around 200 g of precipitated silica can be produced and, if it is assumed that 70 % of sodium hydroxide can be recovered, the sodium hydroxide needed is only 83 g. The process will be more competitive if the CO₂ source is the flue gas of the combustion process.

CONCLUSIONS

In this paper, sol-gel precipitation using CO₂ impregnation and mechanical fragmentation has successfully been applied to produce precipitated silica from POMFA. The optimum condition for precipitating 600 cm³ of silica extract which has a silica content of 5.5% (m/v) and a mol ratio of silica to Na₂O of 1.1 was a stirring speed of 882 RPM and CO₂ flow rate of 88 cm³/min. The CO₂ needed for the sol-gel precipitation process was 4886±56 cm³. The d₅₀ of the precipitated silica particle size of 10.67±1.44 μm can be obtained by a wet crushing process using a household blender. The BET specific surface area of the precipitated silica obtained can be tailored by varying the pH and the temperature of the precipitation process. The SSA of the precipitated silica obtained was in the range of 50 – 140 m²/g. The characteristics of typical precipitated silica obtained, which were analyzed using FTIR, SEM, SEM-EDS and XRD, match the characteristics of the silica from other references obtained at the laboratory level.

ACKNOWLEDGEMENTS

This work was financially supported by the Graduate School of the Prince of Songkla University. The author received a scholarship for his graduate degree from DGHE Indonesia.

REFERENCES

Affandi, S., Setyawan, H., Winardi, S., Purwanto, A., and Balgis, R., A Facile Method for Production of High-Purity Silica Xerogels from Bagasse Ash, *Advanced Powder Technology*, 20(5), 468-472 (2009). <https://doi.org/10.1016/j.appt.2009.03.008>

- Amin N.U., Khattak S, Noor S, and Ferroze, I., Synthesis and Characterization of Silica from Bottom Ash of Sugar Industry, *J. Clean Prod.*, 117, 207-211 (2016). <https://doi.org/10.1016/j.jclepro.2016.01.042>
- Baldyga, J., Jasin, M., Jodko, K. and Petelski, P., Precipitation of Amorphous Colloidal Silica from Aqueous Solutions—Aggregation Problem, *Chem. Eng. Sci.*, 77, 207-216 (2012). <https://doi.org/10.1016/j.ces.2012.03.046>
- Cai, X., Hong, R.Y., Wang, L.S., Wang, X.Y., Li, H.Z. and Wei, D.G., Synthesis of Silica Powders by Pressured Carbonation, *Chem. Eng. J.*, 151(1-3), 380-386 (2009). <https://doi.org/10.1016/j.cej.2009.03.060>
- Cheng, Y., Xia, M., Luo, F., Li, N., Guo, C. and Wei, C., Effect of Surface Modification on Physical Properties of Silica Aerogels Derived from Fly Ash Acid Sludge, *Colloid Surface A.*, 490, 200-206 (2016). <https://doi.org/10.1016/j.colsurfa.2015.11.055>
- Future Market Insights. <http://www.futuremarketinsights.com/articles/precipitated-silica-market-to-witness-steady-growth-in-brics-owing-to-demand-from-automotive-and-consumer-electronics-market>. [27 December 2015].
- Indexmundi. <http://www.indexmundi.com/agriculture/?commodity=palm-oil&graph=production>. [January 15, 2016].
- Kalpathy, U., Proctor, A. and Shultz, J., A Simple Method for Production of Pure Silica from Rice Hull Ash, *Bioresour. Technol.*, 73(3), 257-262 (2000). [https://doi.org/10.1016/S0960-8524\(99\)00127-3](https://doi.org/10.1016/S0960-8524(99)00127-3)
- Kamath, S.R. and Proctor, A., Silica Gel from Rice Hull Ash: Preparation and Characterization, *Cereal Chem.*, 74(4), 484-487 (1998). <https://doi.org/10.1094/CCHEM.1998.75.4.484>
- Krishnamoorthy, S., Iyer, N.R. and Murthy, A.R., Carbonization on Combustion and Biodegradation of Agricultural Waste as a Possible Source of Silica, *Appl. Biochem. Biotechnol.*, 175(3), 1622-1632 (2015). <https://doi.org/10.1007/s12010-014-1362-8>
- Martinez, J.R., Palomares, S., Ortega-Zarzosa, G., Ruiz, F. and Chumakov, Y., Rietveld Refinement of Amorphous SiO₂ Prepared Via Sol-Gel Method, *Mater. Lett.*, 60(29-30), 3526-3529 (2006). <https://doi.org/10.1016/j.matlet.2006.03.044>
- Montgomery, D.C., Design and Analysis of Experiments (5th edn), John Wiley & Sons, New York (2001).
- Musić, S., Filipović-Vinceković, N. and Sekovanić, L., Precipitation of Amorphous SiO₂ Particles and Their Properties, *Braz. J. Chem. Eng.*, 28(1), 89-94 (2011). <https://doi.org/10.1590/S0104-66322011000100011>

- Quarch, K., Durand, E., Schilde, C., Kwade, A. and Klind, M., Mechanical Fragmentation of Precipitated Silica Aggregates, *Chem. Eng. Res. Des.*, 88(12), 1639-1647 (2010). <https://doi.org/10.1016/j.cherd.2010.01.007>
- Rajanna, S.K., Kumar, D., Vinjamur, M. and Mukhopadhyay, M., Silica Aerogel Microparticles from Rice Husk Ash for Drug Delivery, *Ind. Eng. Chem. Res.*, 54(3), 946-956 (2015). <https://doi.org/10.1021/ie503867p>
- Ramos-de-la-Pena, A.M., Catherine, M.G.C., Renard, C.M.G.C., Wicker, L., Montañez, J., María de la Luz Reyes-Vega, M.L. and Contreras-Esquivel, J.C., Optimization of the Liquefaction and Saccharification of Structural Polysaccharides of Jicama (*Pachyrhizuserosus L.*) Tissue by Enzymatic Pulping, *LWT-Food Sci. Technol.*, 46(1), 232-238 (2012). <https://doi.org/10.1016/j.lwt.2011.10.001>
- Rozainee, M., Ngo, S.P., Salema, A.A. and Tan, K.G., Fluidized Bed Combustion of Rice Husk to Produce Amorphous Siliceous Ash, *Energy Sustain. Dev.*, 12(1), 33-42 (2008). [https://doi.org/10.1016/S0973-0826\(08\)60417-2](https://doi.org/10.1016/S0973-0826(08)60417-2)
- Sardeing, R., Aubin, J. and Xuereb, C., Gas-Liquid Mass Transfer: A Comparison of Down and Up Pumping Axial Flow Impellers with Radial Turbines, *Trans IChemE*, 82(A12), 1589-1596 (2004). <https://doi.org/10.1205/cerd.82.12.1589.58030>
- Schlomach, J. and Kind, M., Investigations on the Semi-Batch Precipitation of Silica, *J. Colloid Interf. Sci.*, 277(2), 316-326 (2004). <https://doi.org/10.1016/j.jcis.2004.04.051>
- Shim, J., Velmurugan, P., and Ohb, B.T., Extraction and Physical Characterization of Amorphous Silica Made from Corn Cob Ash at Variable pH Conditions Via Sol Gel Processing, *J. Ind. Chem. Eng.*, 30, 249-253 (2015). <https://doi.org/10.1016/j.jiec.2015.05.029>
- Sing, K.S.W., Everett, D.H., Haul, R.A.W., Moscou, L., Pierotti, R.A., Rouquerol, J., and Siemieniewska, T., Reporting Physisorption Data for Gas/Solid Systems with Special Reference to the Determination of Surface Area and Porosity, *Pure & App. Chem.*, 57(4), 603-619 (1985).
- Srinivasan, V., Kullagounder, S., Srinivasan, S., and Thiraviyam, S., Synthesis of esoporous Silicon with Uniform Pore Size Using the Ashes of Husks from Panicum Miliare Millet: A Novel Recyclable Bio-Waste, *Silicon*, 2015, 1-7 (2015). <https://doi.org/10.1007/s12633-015-9321-8>
- Subbukrishna, D.N., Suresh, K.C., Paul, P.J., Dasappa, S. and Rajan, N.K.S., Precipitated Silica from Rice Husk Ash by IPSIT Process. 15th European Biomass Conference & Exhibition. Berlin (2007).
- Tay, J.H. and Show, K.Y., Use of Ash Derived from Oil-Palm Waste Incineration as A Cement Replacement Material. *Resources, Conservation and Recycling*, 13(1), 27-36 (1995). [https://doi.org/10.1016/0921-3449\(94\)00012-T](https://doi.org/10.1016/0921-3449(94)00012-T)
- Utama, P.S., Yamsaengsung, R. and Sangwichien, C., Precipitated Silica Derived From Palm Oil Mill Fly Ash: Kinetics And Characterization, *Key Eng. Mater.*, 673, 183-192 (2016). <https://doi.org/10.4028/www.scientific.net/KEM.673.183>
- Zemnukhova, L.A., Egorov, A.G., Fedorishcheva, G.A., Barinov, N.N., Sokol'nitskaya, T.A. and Botsul, A.I., Properties of Amorphous Silica Produced from Rice and Oat Processing Waste, *Inorg. Mater.*, 42(1), 24-29 (2006). <https://doi.org/10.1134/S0020168506010067>